Fritz, R., Alzate-Morales, J. H., Spencer, J., Mulholland, A. J., & Van Der Kamp, M. W. (2018). Multiscale simulations of clavulanate inhibition identify the reactive complex in class A β-lactamases and predict efficiency of inhibition. *Biochemistry*. https://doi.org/10.1021/acs.biochem.8b00480

Multiscale Simulations of Clavulanate Inhibition Identify the reactive Complex in Class A β-lactamases and Predict Efficiency of Inhibition

Rubén A. Fritz[a], Jans H. Alzate-Morales[a*], James Spencer[b], Adrian J. Mulholland[c*] and Marc W. van der Kamp[c,d*]

[a] Center for Bioinformatics and Molecular Simulations, Faculty of Engineering, University of Talca, Talca, Chile.

[b] School of Cellular and Molecular Medicine, University of Bristol, University Walk, Bristol, BS8 1TD, UK.

[c] Centre for Computational Chemistry, School of Chemistry, University of Bristol, Cantock's Close, Bristol, BS8 1TS, UK.

[d] School of Biochemistry, University of Bristol, University Walk, Bristol, BS8 1TD, UK; marc.vanderkamp@bristol.ac.uk, Tel: +44 117 331 2147, Fax: +44 17 331 2168.

ABSTRACT: Clavulanate is used as an effective drug in combination with β-lactam antibiotics to treat infections of some antibiotic resistant bacteria. Here, we perform combined quantum mechanics / molecular mechanics simulations of several covalent complexes of clavulanate with class A β-lactamases KPC-2 and TEM-1. Simulations of the deacylation reactions identify the decarboxylated trans-enamine complex as responsible for inhibition. Further, the obtained free energy barriers discriminate clinically relevant inhibition (TEM-1) from less effective inhibition (KPC-2).

Antibiotic resistance is one of the greatest global threats to human health.[1] Resistance to almost every class of clinically approved antibiotic has been observed.[2,3] The increase and global spread of bacterial antimicrobial resistance limits treatment options and affects many aspects of medicine, from cancer to organ transplants. In the worst case, no effective treatment may be available for bacterial infections.[4,5] β-lactam antibiotics are a mainstay of modern medicine but suffer from increasing resistance in bacteria. β-lactamase enzymes are the key source of resistance for many human pathogens (particularly Gram-negative bacteria).[2] Inhibitors of these enzymes are clinically important: given in conjunction with β-lactam antibiotics, they can restore the effectiveness of the antibiotic. Only five β-lactamase inhibitors are currently clinically approved: clavulanate (CLA), sulbactam (SUL), tazobactam (TAZ) and the non-β-lactam agents avibactam (AVI) and vaborbactam (VAB); and resistance to them is also increasing.[6–11] Discovery and development of new compounds with this type of biological activity is necessary to combat antibiotic resistance and to recover the usefulness of β-lactam antibiotics.[12]

β-lactam antibiotics are covalent inhibitors of bacterial DD-trans-peptidases.[12] β-lactamases inactivate β-lactams by hydrolyzing the amide bond of the four-membered β-lactam ring, in serine β-lactamases (SBLs) via a transient covalent acylenzyme intermediate. β-lactamase inhibitors also bind covalently to SBLs[12] but the inhibitor remains covalently attached to the active site serine, preventing the enzyme from turning over.[13–15] Crucially, to be effective, the rate of breaking this bond must be slow. Research on covalent drugs has increased in recent years due e.g. to the possibility of prolonged residence times. Successful examples include covalent inhibitors of kinases.[16,17] *In-silico* methods, such as docking and quantitative structure-activity relationship models, can play an important role in designing and developing covalent drugs. To understand reactivity and specificity of covalent binders to protein targets, and related drug resistance[18], combined quantum mechanics/molecular mechanics (QM/MM) methods are a highly promising approach.[15,19–21]

Acylation of SBLs by β-lactamase inhibitors is likely to occur with the same mechanism as for β-lactam antibiotics such as benzyl-penicillin (Figs. S1).[22] In class A β-lactamases, the most widespread SBLs, deacylation consists of proton abstraction from a conserved water molecule (deacylating water, DW) by Glu166, and nucleophilic attack by DW on the ester carbon of the acyl–enzyme complex (AEC) with subsequent release of the inactivated antibiotic.[23] Carbapenems that inhibit β-lactamases show a stable AEC,[19] thus the rate of deacylation is central to activity. In the case of inhibitors, after the AEC is formed and depending on the properties of the β-lactamase and inhibitor, the reaction will proceed to deacylation (Fig. S1-S3) or irreversible inactivation[6] (i.e. formation of one of several proposed protein-ligand covalent complexes or

adducts). Then, opening of the five-membered ring of the β-lactam inhibitor (CLA, TAZ or SUL) AEC leads to formation of a transient imine intermediate, which rearranges to form an enamine species, in either a *trans* or a *cis* conformation.[6,24] Ultimately, a stable covalent complex is reached and a slow hydrolysis or deacylation rate is observed (Fig S5). Irreversible inhibition is possible when a *trans*-enamine decarboxylated complex (TEDC) for CLA, or a *trans*-enamine complex (TEC) in the case of SUL and TAZ, is formed. An aldehyde complex (ADEC) can also be reached by consecutive reactions of the *cis*-enamine[6,24] (Fig. S3-S4). Specifically, TEDC and TEC have been trapped and characterized through X-ray and Raman spectroscopy experiments in complex with SHV-1 β-lactamase and mutants thereof.[25–29]

Among the Class A β-lactamases, TEM-1 and KPC-2 are well studied and clinically important enzymes that in addition to differences in specificity towards substrates are distinguished by differing susceptibilities to inhibition by CLA. Both enzymes hydrolyze the inhibitor, but at different rates (k_{cat} in Table 1). This feature translates into KPC-2 resistance to CLA action. TEM-1 and KPC-2 also show distinct inactivation rates as measured by their respective k_{inact} values (Table 1).[6,7] While, in general, the k_{inact}/K_i ratio is the most effective measure of irreversible inhibition[30] as inclusion of K_i values accounts for effects on both acylation and deacylation rates, in this instance k_{inact} alone can effectively report irreversible inhibition by CLA of TEM-1 and KPC-2 as deacylation is the more important and limiting step in inhibition. In this case CLA is a substantially less effective inhibitor of KPC-2 than TEM-1, making infections by KPC-2 producing bacteria insusceptible to treatment by β-lactam/CLA combinations.[6,7]

A QM/MM protocol, modelling the first step of deacylation in Class A β-lactamases, was developed by Chudyk *et al.,* and shown to be an effective computational 'assay' for carbapenemase activity of class A β-lactamases.[19] With SCC-DFTB[31] as QM method, enzymes inhibited by carbapenems showed barriers of 17-18 kcal/mol for the first deacylation step, whereas non-inhibited enzymes showed a significantly lower barriers (≤ 10 kcal/mol). The simulations thus correctly discriminated between β-lactamases with carbapenemase activity and those without. Here, we apply a similar simulation protocol to study deacylation of covalent β-lactamase-inhibitor complexes. We calculate activation free energies for deacylation ($\Delta^{\ddagger}G_{calc}$), for the different covalent complexes TEDC, ADEC and AEC (used as a control calculation for the screening method) formed between CLA and Class A β-lactamases TEM-1 and KPC-2 (Fig S4). Our aim was to identify the complexes responsible for irreversible inhibition and to illustrate that the QM/MM screening methodology can be extended to predict inhibition of Class A β-lactamases by other molecules of interest.

Class A β-lactamase crystal structures of TEDC, ADEC and AEC complexes were used to build these into TEM-1 (PDB: 1BTL) and KPC-2 (PDB: 2OV5), retaining the structurally conserved deacylating water (DW). The models were structurally refined and the adduct prepared for QM/MM simulation using a MM relaxation protocol (details in ESI; adduct parameters at DOI: 10.6084/m9.figshare.6301976). Thereafter, 50 ps of QM/MM production MD was performed without restraints prior to each reaction simulation, to generate independent starting points. The DW, Ser70-adduct and sidechain of Glu166, from its Cβ atom, were selected as the quantum mechanical (QM) region (**Figure 1**), which was described with SCC-DFTB,[31] while the rest of the system was treated with the ff14SB[32] MM force field. (see ESI for details). End points of this equilibration were checked for geometrical consistency for the deacylation reaction by examining the key catalytic distances. Reaction coordinates were defined as previously[19,23] (**Figure 1**).

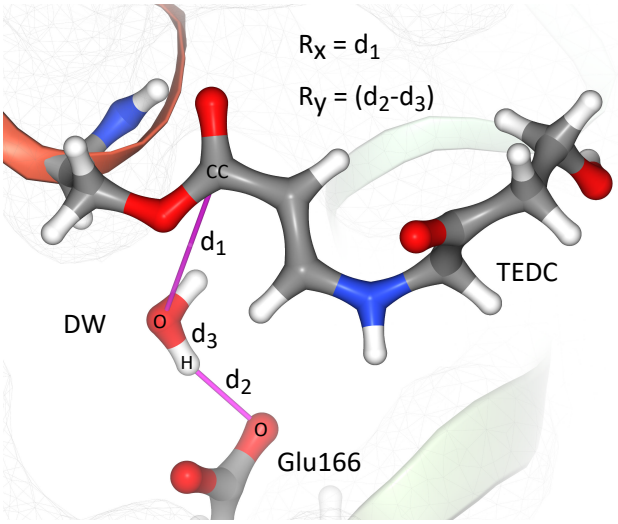

Figure 1. Reaction Coordinates used for umbrella sampling MD simulations of the reactions. QM atoms are depicted as hyperballs with NGLview.[33]

Complete 2D-energy surfaces were then obtained by QM/MM Umbrella Sampling (US) simulations along the two defined reaction coordinates and using the weighted-histogram analysis method (WHAM; details in ESI, see **Figure 2**, **Figures S5-S22**). The minimum free energy path (MEP) on the surfaces was determined using the Minimum Energy Pathway Analysis for energy landscapes (MEPSA) software.[34] The highest point along the MEP was taken as the transition state energy to obtain $\Delta^{\ddagger}G_{calc}$. Three series of US simulations, with different starting points as taken from the unbiased QM/MM MD runs were performed to test convergence of $\Delta^{\ddagger}G_{calc}$.

Summarized $\Delta^{\ddagger}G_{calc}$ and relative free energy differences $\Delta\Delta^{\ddagger}G$ ($\Delta^{\ddagger}G^{KPC-2} - \Delta^{\ddagger}G^{TEM-1}$) values for the different enzyme CLA-adducts are reported in **Table 1**. The calculated deacylation rates for the AEC and ADEC for KPC-2 and TEM-1 are equal for these adducts ($\Delta\Delta^{\ddagger}G$ values are less than the cumulative standard deviation) and are of the same order of magnitude as those reported by Chudyk *et al.* [19] for deacylation of carbapenem AECs by carbapenem-hydrolyzing class A β-lactamases.[21] This suggests that neither the AEC nor ADEC complex is responsible for irreversible inhibition (**Table 1**).[7,35] In contrast, the $\Delta^{\ddagger}G_{calc}$ values for the TEDCs in KPC-2 and TEM-1, differ substantially from those for the AEC or ADEC, identifying a markedly higher barrier for deacylation and strongly supporting the contention that the TEDC is the covalent complex responsible for irreversible inhibition.[6,7,24] Moreover, these values agree well with those derived from the respective experimental inactivation constants (k_{inact}, the parameter primarily related to the loss of enzyme activity).[7,35] Importantly, our computational approach also differentiates the two enzymes ($\Delta\Delta^{\ddagger}G$ value −5.1 kcal/mol); distinguishing efficient inhibition of TEM-1 from less effective inhibition of KPC-2 and so replicating what is observed both in *in vitro* experiments and in the clinic.

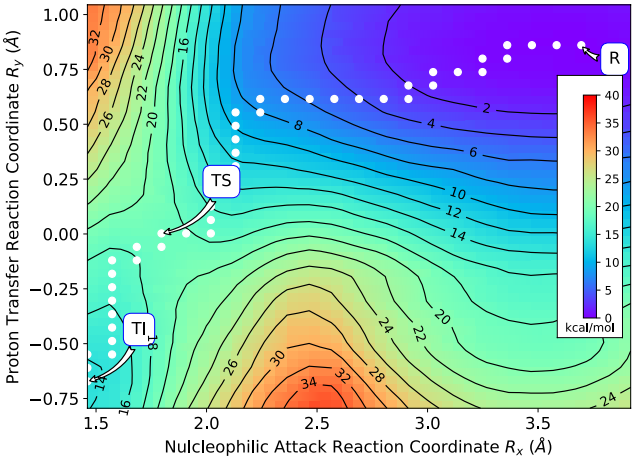

Figure 2. Free Energy Surface for the first step of deacylation of TEDC in KPC-2. R = reactants (KPC-2, TEDC and DW), TS = "Transition State", TI = Tetrahedral Intermediate of the first step of deacylation. White dots represent the MEP of the reaction.

Table 1. Experimental ($\Delta^{\ddagger}G_{exp}$) and calculated free energies of activation ($\Delta^{\ddagger}G_{calc}$) for the first step of deacylation of TEDC, ADEC and AEC; and kinetics parameters. $\Delta^{\ddagger}G_{calc}$ barriers are the average from three simulations with standard deviations.

β-lactamase	k_{inact} (s^{-1})	$\Delta^{\ddagger}G_{exp}$ (kcal/mol)	k_{cat} (s^{-1})	$\Delta^{\ddagger}G_{exp}$ (kcal/mol)	$\Delta^{\ddagger}G_{calc}$ (kcal/mol)		
					TEDC	ADEC	AEC
KPC-2	0.027[7]	19.7	18[36]	15.8	18.7 (0.6)	7.5 (0.4)	8.4 (1.6)
TEM-1	0.0017[35]	21.3	0.21[35]	18.5	23.8 (1.2)	7.4 (0.2)	7.3 (0.9)
$\Delta\Delta^{\ddagger}G$		−1.6		−2.6	−5.1	−0.1	1.1

The KPC-2 TEDC acyl-enzyme simulations indicate slightly shorter hydrogen bonds with the acyl oxygen (donated by the Ser70 and Thr/Ala237 amides) than in TEM-1 (2.12±0.20 Å and 1.86±0.12 Å vs. 2.29±0.24 Å and 1.93±0.13 Å, respectively), which may be related to the distinct conformation of the protein backbone likely imposed by the Cys69-Cys238 disulfide bond (present in KPC-2 only).[37] Apart from this small difference in the acyl-enzyme complexes, simulations do not indicate a clear effect that explains the difference in barrier between TEM-1 and KPC-2 (**Figures S23-S26**). This is consistent with what we have observed previously for carbapenem breakdown in class A beta-lactamases[19]: multiple subtle effects are likely to be in play. The first-principles QM/MM reaction simulations performed here are able to incorporate these subtle effects. Indeed, detailed investigation of reactivity will likely be necessary to understand the origins of differences in the inhibition efficiency of serine β-lactamases with covalent β-lactam inhibitors.

In conclusion, QM/MM reaction simulations were used to calculate $\Delta^{\ddagger}G_{calc}$ for the first deacylation step in β-lactamases with three different CLA adducts; the acyl, aldehyde and decarboxylated *trans*-enamine enzyme complexes. The higher activation free energies for deacylation of the latter (TEDC) adduct lead us to conclude that this is the complex responsible for irreversible inhibition of both enzymes. We thus show that the QM/MM screening protocol is reliable in discriminating the inhibitory activity of different covalent complexes in class A β-lactamases. Furthermore, the computational screening method is able to differentiate enzymes for which CLA is an effective inhibitor (TEM-1) from those for which it is not (KPC-2). Taken together with our previous results on carbapenem deacylation,[19] these data show that QM/MM simulation protocols assessing likelihood of deacylation in class A β-lactamase AECs are applicable to chemically distinct acylated moieties in different enzymes. QM/MM screening of inhibitory activity against class A β-lactamases could thus help design better β-

lactamase inhibitors as well as β-lactam antibotics, with the possibility of expanding the procedure to other serine β-lactamases (and other serine hydrolases).

ASSOCIATED CONTENT

Supporting Information. Simulation details, reaction mechanisms of clavulanate in KPC-2 and TEM-1 (**Figures S1-S4**), free energy surfaces for all reactions simulated (**Figures S5–S22**), representative structures (**Figures S23-S26**). The Supporting Information is available free of charge on the ACS Publications website.

AUTHOR INFORMATION

Corresponding Authors.

Jans H. Alzate-Morales, email: jalzate@utalca.cl

Adrian J. Mulholland, email: adrian.mulholland@bristol.ac.uk

Marc W. Van der Kamp, email: marc.vanderkamp@bristol.ac.uk

Author Contributions

MWK & AJM designed the study; RAF performed and analyzed all simulations, with help from MWK. All authors contributed to writing the manuscript.

ACKNOWLEDGMENT

RAF thanks the Royal Society of Chemistry (RSC) for the Researcher Mobility Grant awarded in 2016 and the University of Talca for a PhD scholarship. RAF and JAM knowledge the financial support through project FONDECYT No. 1140618. AJM thanks EPSRC for support (EP/M027546/1 and EP/022609/1). MWK is a BBSRC David Phillips Fellow (BB/M026280/1). This work was conducted using the computational facilities of the Advanced Computing Research Centre, University of Bristol.

REFERENCES

(1) Zaman, S. Bin, Hussain, M. A., Nye, R., Mehta, V., Mamun, K. T., and Hossain, N. (2017) *Cureus 9*.

(2) Fair, R. J., and Tor, Y. (2014) *Perspect. Medicin. Chem.* 25–64.

(3) Munita, J. M., Arias, C. A., (2016) Mechanisms of Antibiotic Resistance. *Microbiol Spectr. 4*, 1–37.

(4) van Duin, D., and Paterson, D. L. (2016) *Infect. Dis. Clin. North Am. 30*, 377–390.

(5) Cerceo, E., Deitelzweig, S. B., Sherman, B. M., and Amin, A. N. (2016) *Microb. Drug Resist. 22*, 412–431.

(6) Drawz, S. M., and Bonomo, R. a. (2010) *Clin. Microbiol. Rev. 23*, 160–201.

(7) Papp-Wallace, K. M., Bethel, C. R., Distler, A. M., Kasuboski, C., Taracila, M., and Bonomo, R. A. (2010) *Antimicrob. Agents Chemother. 54*, 890–897.

(8) Shen, Z., Ding, B., Bi, Y., Wu, S., Xu, S., Xu, X., Guo, Q., and Wang, M. (2017) *Antimicrob. Agents Chemother. 61*, 1–5.

(9) Soroka, D., De La Sierra-Gallay, I. L. I. L., Dubée, V., Triboulet, S. S., Van Tilbeurgh, H., Compain, F., Ballell, L., Barros, D., Mainardi, J. L., Hugonnet, J. E., Arthur, M., Dubée, V., Triboulet, S. S., Van Tilbeurgh, H., Compain, F., Ballell, L., Barros, D., Mainardi, J. L., Hugonnet, J. E., and Arthur, M. (2015) *Antimicrob. Agents Chemother. 59*, 5714–5720.

(10) Winkler, M. L., Papp-Wallace, K. M., Taracila, M. A., and Bonomo, R. A. (2015) *Antimicrob. Agents Chemother. 59*, 3700–9.

(11) Morosini, M. I., Martin, O., Maza, S. De, and Pedrosa, E. G. G. De. (2008) *Clin. Microbiol. Infect. 14*, 53–62.

(12) Worthington, R. J., and Melander, C. (2013) *J. Org. Chem. 78*, 4207–4213.

(13) Singh, J., Petter, R. C., Baillie, T. a, and Whitty, A. (2011) *Nat. Rev. Drug Discov. 10*, 307–317.

(14) Bauer, R. A. (2015) *Drug Discov. Today 20*, 1061–1073.

(15) De Cesco, S., Kurian, J., Dufresne, C., Mittermaier, A. K., and Moitessier, N. (2017) *Eur. J. Med. Chem. 138*, 96–114.

(16) Baillie, T. A. (2016) *Angew. Chemie Int. Ed. 55*, 13408–13421.

(17) Miller, R. M., and Taunton, J. (2014) *Methods Enzymol. 548*, 93–116.

(18) Callegari, D., Ranaghan, K. E., Woods, C. J., Minari, R., Tiseo, M., Mor, M., Mulholland, A. J., and Lodola, A. (2018) *Chem. Sci. 9*, 2740–2749.

(19) Chudyk, E. I., Limb, M. a L., Jones, C., Spencer, J., van der Kamp, M. W., and Mulholland, A. J. (2014) *Chem. Commun. 50*, 14736–9.

(20) De Vivo, M. (2011) *Front. Biosci. 16*, 1619–1633.

(21) Lodola, A., and De Vivo, M. (2012) Chapter 11 - The Increasing Role of QM/MM in Drug Discovery, in *Structural and Mechanistic Enzymology* (Christov, C., and Karabencheva-Christova, T. B. T.-A. in P. C. and S. B., Eds.), pp 337–362. Academic Press.

(22) Hermann, J. C., Hensen, C., Ridder, L., Mulholland, A. J., and Höltje, H.-D. (2005) *J. Am. Chem. Soc. 127*, 4454–4465.

(23) Hermann, J. C., Ridder, L., Höltje, H.-D., and Mulholland, A. J. (2006) *Org. Biomol. Chem. 4*, 206–10.

(24) Wang, D. Y., Abboud, M. I., Markoulides, M. S., Brem, J., and Schofield, C. J. (2016) *Future Med. Chem. 8*, 1063–1084.

(25) Helfand, M. S., Totir, M. A., Carey, M. P., Hujer, A. M., Bonomo, R. A., and Carey, P. R. (2003) *Biochemistry 42*, 13386–13392.

(26) Totir, M. a, Padayatti, P. S., Helfand, M. S., Carey, M. P., Bonomo, R. a, Carey, P. R., and van den Akker, F. (2006) *Biochemistry 45*, 11895–11904.

(27) Miani, A., Helfand, M. S., and Raugei, S. (2009) *J. Chem. Theory Comput. 5*, 2158–2172.

(28) Padayatti, P. S., Helfand, M. S., Totir, M. A., Carey, M. P., Hujer, A. M., Carey, P. R., Bonomo, R. A., and van den Akker, F. (2004) *Biochemistry 43*, 843–848.

(29) Kalp, M., Totir, M. A., Buynak, J. D., and Carey, P. R. (2009) *J. Am. Chem. Soc. 131*, 2338–2347.

(30) Holdgate, G. A., Meek, T. D., and Grimley, R. L. (2017) *Nat. Rev. Drug Discov. 17*, 115.

(31) Elstner, M., Porezag, D., Jungnickel, G., Elsner, J., Haugk, M., Frauenheim, T., Suhai, S., and Seifert, G. (1998) *Phys. Rev. B 58*, 7260–7268.

(32) Maier, J. A., Martinez, C., Kasavajhala, K., Wickstrom, L., Hauser, K. E., and Simmerling, C. (2015) *J. Chem. Theory Comput. 11*, 3696–3713.

(33) Nguyen, H., Case, D. A., and Rose, A. S. (2017) *Bioinformatics* btx789-btx789.

(34) Marcos-Alcalde, I., Setoain, J., Mendieta-Moreno, J. I., Mendieta, J., and Gómez-Puertas, P. (2015) *Bioinformatics 31*, 3853–3855.

(35) Thomas, V. L., Golemi-Kotra, D., Kim, C., Vakulenko, S. B., Mobashery, S., and Shoichet, B. K. (2005) *Biochemistry 44*, 9330–9338.

(36) Papp-Wallace, K. M., Taracila, M. A., Smith, K. M., Xu, Y., and Bonomo, R. A. (2012) *Antimicrob. Agents Chemother. 56*, 4428–4438.

(37) Fonseca, F., Chudyk, E. I., van der Kamp, M. W., Correia, A., Mulholland, A. J., and Spencer, J. (2012) *J. Am. Chem. Soc. 134*, 18275–18285.

"For Table of Contents Use Only"